Available online at www.sciencedirect.com
ScienceDirect
International Journal of Heat and Fluid Flow 29 (2008) 48–61
International Journal of HEAT AND FLUID FLOW
www.elsevier.com/locate/ijhff

Assessment of intermittency transport equations for modeling transition in boundary layers subjected to freestream turbulence

Keerati Suluksna, Ekachai Juntasaro *

School of Mechanical Engineering, Institute of Engineering, Suranaree University of Technology, Nakhon Ratchasima 30000, Thailand

Received 2 May 2006; received in revised form 30 June 2006; accepted 8 August 2007
Available online 23 October 2007

Abstract

The γ–Re_θ transition model of Menter et al. [Menter, F.R., Langtry, R.B., Volker, S., Huang, P.G., 2005. Transition modelling for general purpose CFD codes. ERCOFTAC International Symposium Engineering Turbulence Modelling and Measurements] is a highly generalized transport equation model in which it has been developed based on the concept of local variables compatible with modern CFD methods where the unstructured grid and the parallel computing technique are usually integrated in. To perform the prediction with this model, two essential parameters, F_{length} which is used to control the length of the transition region and $Re_{\theta c}$ which is used to control the onset of the transition location, must be specified to close the model. At present, both parameters are proprietary and their formulations are unpublished. For the first time here, the relations for both parameters are formulated by means of numerical experiments and analysis under the assumption of $Re_{\theta c} = Re_{\theta t}$ corresponding with the bypass transition behavior. Based on this analysis, the optimized values of the parameters are found and their relations can be constructed as follows: $Re_{\theta c} = 803.73(Tu_{\infty,\text{le}} + 0.6067)^{-1.027}$ and $F_{\text{length}} = 163\ln(Tu_{\infty,\text{le}}) + 3.625$. The performance of this transition model is assessed by testing with the experimental cases of T3AM, T3A, and T3B. Detailed comparisons with the predicted results by the transition models of Suzen and Huang [Suzen, Y.B., Huang, P.G., 2000. Modeling of flow transition using an intermittency transport equation. J. Fluids Eng. 122, 273–284] and Lodefier et al. [Lodefier, K., Merci, B., De Langhe, C., Dick, E., 2003. Transition modelling with the SST turbulence model and intermittency transport equation. ASME Turbo Expo, Atlanta, GA, USA, June 16–19], and also with the predicted results by the k–ε model of Launder and Sharma [Launder, B.E., Sharma, B., 1974. Application of the energy dissipation model of turbulence to the calculation of flow near a spinning disk. Letters in Heat and Mass Transfer 1, 131–138] and the SST model of Menter [Menter, F.R., 1994. Two-equation eddy-viscosity turbulence models for engineering applications. AIAA 32, 1598–1605] are presented here. Results show that the proposed relations for F_{length} and $Re_{\theta c}$ can work well with the model to give good agreement in predicting the transition.

Keywords: Transition; Intermittency; Boundary layer; Freestream turbulence; Bypass; Modeling; Zero pressure gradient

1. Introduction

Flow transition plays an important role in the design and performance of turbomachinery applications and aerospace devices where the wall shear stress or the wall heat transfer or a combination of both is of interest. Majority of boundary layer flows in turbomachines and aerospace devices involve the flow transition under the effects of various factors, such as freestream turbulence, pressure gradient and separation, Reynolds number, Mach number, turbulent length scale, wall roughness, streamline curvature, heat transfer, etc. (Suzen and Huang, 2001). For example, the influence of transition on engineering applications is the boundary layer on the blade, particularly in low pressure turbine applications, where the flow in the cascade passage can be laminar and transitional over 50–70% of the blade surface (Lardeau and Leschziner, 2005). Typically, the transition over the blade surface and the change in the properties related to the transition process can have a

* Corresponding author. Tel.: +66 89 8971657; fax: +66 44 224613.
E-mail addresses: junta@g.sut.ac.th, junta@sut.ac.th, e_juntasaro@hotmail.com (E. Juntasaro).

0142-727X/$ - see front matter © 2007 Elsevier Inc. All rights reserved.
doi:10.1016/j.ijheatfluidflow.2007.08.003

strong influence on the operation and performance. It has been known that early transition can prevent the separation (stall) of the suction-side boundary layer and consequently lead to a significant reduction in total-pressure loss. As a result, the number of blades and stages can be reduced in turbomachines to save cost. Furthermore, in case of aerospace devices, the transition process can also have a large effect on the performance of airfoils and bluff bodies because of the separation behavior of boundary layers. For example, at low Reynolds number with low freestream turbulence, the boundary layer on the airfoil surface has a tendency to remain laminar and hence the flow may separate before it becomes turbulent. This can reduce the efficiency and result in an increase of fuel consumption. For all these reasons, the performance, weight and cost associated with turbomachines and aerospace devices can be affected by transition and the prediction of its behavior is an important element in analysis and performance evaluation and ultimately in the design of more efficient system (Langtry and Menter, 2005).

In general, transition in a boundary layer on a flat plate with zero pressure gradient can be divided into two different basic modes: *natural* and *bypass* modes. The natural transition process occurs at low freestream turbulence levels (less than 1%). The process of this transition gradually appears after a critical value of the Reynolds number is exceeded. An instability in the laminar boundary layer is developed in the form of two-dimensional Tollmien–Schlichting (T–S) waves (linear instability). This instability becomes three-dimensional and non-linear by the formation of vortex loops and there appears the formation of turbulent spots in the highly fluctuating portion of the flow. These turbulent spots spread laterally downstream until the entire boundary layer is engulfed (Abid, 1993). If the freestream turbulence intensity exceeds 1%, the bypass transition occurs in which case the transition takes place without the appearance of T–S waves. This mechanism is called *bypass* because the linear stage of the transition process is bypassed and disturbances are amplified by a non-linear process. Bypass transition is a complex phenomenon that depends mainly on the freestream turbulence intensity and the status of the boundary layer due to pressure gradient and separation. This process is especially pertinent to the flow over turbine blades, where the freestream turbulence level can reach up to 20% or more (Steelant and Dick, 1996).

At present, there are three main concepts used to model transition in industry. (1) The first approach is based on the stability theory. The successful technique is the so-called e^N method. It is based on the local linear stability theory and the parallel flow assumption in order to calculate the growth of the disturbance amplitude from the boundary layer neutral point to the transition location. This method is not compatible with the current CFD methods because the typical industrial Navier–Stokes solutions are not accurate enough to evaluate the stability equation. In addition, since it is based on the linear stability theory, it cannot predict the transition due to non-linear effects such as high freestream turbulence or surface roughness. Therefore, this method is strictly used for the case of natural transition. (2) The second approach is the use of conventional turbulence models. One way is to switch on the turbulence model, or eddy viscosity, at an experimentally predetermined transition location. This method is *ad hoc* and ignores the transition physics and the importance of the transition zone completely. Especially for flows where the transitional region covers a large portion of the flow field, as observed in many low pressure turbine experiments, this practice can lead to severe errors in the solution. Another way is to use the low Reynolds number turbulence models. However, the ability of low Reynolds turbulence models to predict transition seems to be questionable. This is because the calibration of the damping functions is based on reproducing the viscous sublayer behavior, not on predicting transition from laminar to turbulent flow (Menter et al., 2005). This concluding remark has been proven by many research groups for the last ten years by testing a large variety of turbulence models and comparing the model performance in predicting the transitional flow experiments. The conclusions indicate that most two-equation turbulence models, even the Launder and Sharma (1974) model which was found to be the best performer in predicting transition, gave unsatisfactorily the too early transition onset point and the too short transition length. That shows the inefficiency of the two-equation turbulence models in predicting transition, and, in order to correctly predict the flow affected by transition, some special treatments are needed in turbulence models (Baek and Chung, 2001). (3) The third approach to predict transition, which is favored by the gas turbine industry, is to use the concept of intermittency to blend the flow from laminar to turbulent regions. The intermittency is the fraction of time that the flow is turbulent during the transition phase, which is zero in the laminar region and becomes unity in the fully turbulent region, so that the start and development of transition can be controlled by the intermittency. From experimental observations, the development of intermittency is quite general for the steady boundary layer on a flat plate and therefore the onset location and growth rate of transition can be correlated. For the onset location, most correlations usually relate the freestream turbulence intensity, Tu_∞, and the pressure gradient to the transition momentum thickness Reynolds number. A typical correlation is that of Mayle (1991), which is based on a large number of experimental observations. Another popular correlation is the model of Abu-Ghannam and Shaw (1980), which additionally accounts for the influence of the pressure gradient. The development of transition is usually expressed as a function of the intermittency factor such as the law of Dhawan and Narasimha (1958).

In previous work, the development of intermittency is described algebraically by the Dhawan–Narasimha law and the onset and end of transition are determined by the correlation. However, this law is not appropriate for general applications, which are mostly under the effects of non-zero pressure gradients and high freestream turbu-

lence levels, because it is valid only for the flow with zero pressure gradient and natural transition. The intermittency can more generally be obtained as a solution of the intermittency transport equation. For example, the intermittency transport model of Steelant and Dick (1996) is derived from the intermittency distribution of Dhawan and Narasimha (1958) along the streamline direction. Another example is based on the concept of local variables which is formulated by Menter et al. (2002) in terms of a generalized intermittency variable. The concept of intermittency can be successfully incorporated with the turbulence model in many ways, such as the framework of Steelant and Dick (1996) in which the intermittency is incorporated into two sets of strongly coupled equations of conditionally averaged Navier–Stokes equations. This approach is too complex and not compatible with current CFD codes in which only one set of Navier–Stokes equations is involved. As a result, transitional flows are mostly modeled within a Reynolds Averaged Navier–Stokes (RANS) framework, and usually linked with the turbulence model by modifying some terms in the turbulence model. For instance, the intermittency obtained from the Dhawan–Narasimhahawan-Narasimha law is incorporated into the turbulence model by Baek and Chung (2001). Other examples are Suzen and Huang (2000), Menter et al. (2005) and Lodefier et al. (2003) who use the transport equation for intermittency incorporated into the turbulence model.

This paper is aimed to test and assess the performance of transition models. Three different intermittency transport equations for modeling the transition are implemented: models of Suzen and Huang (2000), Lodefier et al. (2003) and Menter et al. (2005). Two untold parameters F_{length} and $Re_{\theta c}$ which belong to the model of Menter et al. (2005) are formulated by using numerical experiments to close the model. All models are employed to predict the flat plate boundary layer with a shape leading edge under zero pressure gradient and various freestream turbulence intensities. The performance of the models considered is assessed by comparison with the experimental data of the skin friction coefficient, the shape factor and the velocity profile and also with the results obtained from the k–ε turbulence model of Launder and Sharma (1974) and the SST turbulence model of Menter (1994).

2. Transport models for intermittency

Three different transition models based on the concept of intermittency are evaluated: models of Suzen and Huang (2000), Lodefier et al. (2003) and Menter et al. (2005). All models are used in conjunction with the SST turbulence model of Menter (1994). Details of the models are described as follows:

2.1. Transport model of Suzen and Huang (2000)

This intermittency model combining the best features of two existing transition models: models of Cho and Chung (1992) and Steelant and Dick (1996). The first one was derived to simulate the intermittency for the turbulent free shear flows while the other one was derived from the Dhawan–Narasimha law to simulate the near-wall intermittency affected by the turbulent spots during the transition. Additionally, the first one was designed for turbulent free shear flows and hence a realistic variation of the intermittency in the cross-stream direction was adopted, and the other one was used to produce a realistic variation of the intermittency in the streamwise direction.

The transport equation for the intermittency, γ, can be written as

$$\frac{\partial \rho u_j \gamma}{\partial x_j} = (1-\gamma)\left[(1-F)2C_0\rho(u_k u_k)^{1/2}\cdot f(s)f'(s) + F\left(C_1\gamma\frac{P_k}{k} - C_2\gamma\rho\frac{k^{3/2}}{k\omega}\frac{u_i}{(u_k u_k)^{1/2}}\frac{\partial u_i}{\partial x_j}\frac{\partial \gamma}{\partial x_j}\right)\right] + C_3\rho\frac{k^2}{k\omega}\frac{\partial \gamma}{\partial x_j}\frac{\partial \gamma}{\partial x_j} + \frac{\partial}{\partial x_j}\left[(1-\gamma)(\gamma\sigma_{\gamma l}\mu + \sigma_{\gamma t}\mu_t)\frac{\partial \gamma}{\partial x_j}\right], \tag{1}$$

where ρ is the density, u_j is the velocity vector, μ is the dynamic viscosity, μ_t is the eddy viscosity, k is the turbulence kinetic energy, ω is the specific turbulence dissipation rate, P_k is the production term of k and F is the blending factor. The function $f(s)$ is formulated to account for the distributed breakdown. This function depends on the streamline coordinate, s, which can simply be computed by solving its transport equation as follows:

$$\frac{\partial \rho u_j s}{\partial x_j} = \rho(u_k u_k)^{1/2} + \frac{\partial}{\partial x_j}\left[\left(\frac{\mu+\mu_t}{\sigma_s}\right)\frac{\partial s}{\partial x_j}\right]. \tag{2}$$

The model constants are $\sigma_{\gamma l} = \sigma_{\gamma t} = 1.0$, $\sigma_s = 0.1$, $C_0 = 1.0$, $C_1 = 1.6$, $C_2 = 0.16$ and $C_3 = 0.15$. The transition onset location is determined from the correlation which is expressed in terms of the freestream turbulence intensity at the onset, $Tu_{\infty,t}$, and the acceleration parameter, $K_t = (\mu/\rho U_{\infty,t}^2)(\mathrm{d}U_\infty/\mathrm{d}x)_t$:

$$Re_{\theta t} = (120 + 150 Tu_{\infty,t}^{-2/3})\coth[4(0.3 - 10^5 K_t)]. \tag{3}$$

The intermittency is incorporated in the computation by multiplying the eddy viscosity in the diffusion part of the mean flow equation, which is obtained from the turbulence model, by the intermittency factor:

$$\tilde{\mu}_t = \gamma\mu_t. \tag{4}$$

The computation steps are given as follows: (a) solve the mean flow equations: the momentum equations with a modified eddy viscosity, $\tilde{\mu}_t$, and the continuity equation, (b) solve the turbulence model: the k- and ω-equations and then compute the μ_t, (c) compute the onset location of transition, s_t, by searching for the point where $Re_\theta = Re_{\theta t}$, (d) solve the streamline coordinate: the s-equation, and (e) solve the transition model: the γ-equation. During the iteration, it should be noted that keeping γ between 0.01 and 0.99 is necessary to avoid the singularity.

The boundary conditions for the intermittency factor at freestream, outlet and no-slip walls are the zero flux ($\partial\gamma/\partial n = 0$). At inlet, the fixed small value is applied ($\gamma = 0.01$ is recommended and used in this work). The initial condition is set equal to the inlet value. For the streamline coordinate, the boundary conditions are the zero normal gradient ($\partial s/\partial n = 0$) at all boundaries. For the initial conditions, in the region before the onset of transition, $s = s_t$ is applied, and $s = 0$ is used in the rest of the flow field.

2.2. Transport model of Lodefier et al. (2003)

This model was developed specifically for the unsteady transition prediction by modifying the steady transition model with the time dependent behavior of the intermittency equation. The model is based on the concept of two intermittencies affecting the transition: (1) the freestream intermittency, ζ, arising from the diffusion of the turbulent eddies from the freestream to the underlying pseudo-laminar boundary layer to account for the freestream effect and (2) the near-wall intermittency, γ, arising from the turbulent spots during the transition to account for the near-wall effects.

The transport equations for the freestream and near-wall intermittencies can be written as

$$\frac{\partial \rho u_j \zeta}{\partial x_j} = -C_3 \mu_\zeta \frac{U}{U_\infty^2}\frac{\partial U}{\partial n}\frac{\partial \zeta}{\partial n} + \frac{\partial}{\partial x_j}\left[\left(\mu + \frac{\mu_t}{\sigma_\zeta}\right)\frac{\partial \zeta}{\partial x_j}\right], \tag{5}$$

$$\frac{\partial \rho u_j \gamma}{\partial x_j} = 2\rho\beta(1-\tau)[-\ln(1-\gamma)]^{1/2} \cdot [U_\infty F_s + (U f_\tau - U_\infty)(2 - F_s)] + \frac{\partial}{\partial x_j}\left[\left(\mu + \frac{\mu_t}{\sigma_\gamma}\right)\frac{\partial \gamma}{\partial x_j}\right], \tag{6}$$

where τ is the turbulence weighting factor (where $\tau = \zeta + \gamma$), U_∞ is the freestream velocity, U is the local velocity magnitude, f_τ is the model damping function and β is the spot growth rate parameter. The diffusion coefficient μ_ζ is used to control the diffusion of intermittency arising from the freestream. The starting function F_s is used to control the unsteady state in transition.

The model constants are $\sigma_\gamma = \sigma_\zeta = 1.0$ and $C_3 = 15.0$. The onset of transition is determined by the Mayle (1991) correlation which is proportional to the freestream turbulence intensity at the leading edge:

$$Re_{\theta t} = 420 Tu_{\infty,\mathrm{le}}^{-0.69}. \tag{7}$$

With this model, the intermittency is taken into account in the computation by multiplying the eddy viscosity obtained from the SST turbulence model by the turbulence weighting factor τ, whereas, in both k-and ω-equations, the production part, $P_{k/\omega}$, is multiplied by a function of τ as follows:

$$\tilde{\mu}_t = \tau\mu_t, \quad \widetilde{P}_{k/\omega} = \{\tau + (1-\tau)[\max(\mu/\mu_t; 0.1)]\}P_{k/\omega}. \tag{8a, b}$$

The computation steps are summarized as follows: (a) solve the mean flow equations: the momentum equations with a modified eddy viscosity, $\tilde{\mu}_t$, and the continuity equation, (b) solve the turbulence model: the k- and ω-equations with a modified production term $\widetilde{P}_{k/\omega}$, and then compute the μ_t, (c) compute the onset location of transition, x_t, by searching for the point where $Re_\theta = Re_{\theta t}$, (d) solve the transition model: the γ- and ζ-equations. During the iteration, it should be noted that the values of γ and ζ must be kept between 0.0001 and 0.9999 to avoid the singularity.

The boundary conditions for the freestream intermittency at freestream and outlet are the zero flux ($\partial\zeta/\partial n = 0$). At walls, $\zeta = 0$ is applied. At inlet, the value approaching unity is applied ($\zeta = 0.9999$ is recommended and used in this work). For the near-wall intermittency, the boundary conditions at freestream, outlet and walls are the zero flux ($\partial\gamma/\partial n = 0$). At inlet, a small value is applied ($\gamma = 0.0001$ is recommended and used in this work). The initial conditions for both intermittency factors are set to their inlet values all over the flow field.

2.3. Transport model of Menter et al. (2005)

This transition model is based on two transport equations. The first one is the intermittency equation used to trigger the transition process. This equation is developed on the concept of non-zero freestream intermittency, and allows the turbulent eddies from the freestream to disturb the laminar boundary layer. The second equation is formulated in terms of the transition momentum thickness Reynolds number, $Re_{\theta t}$, to avoid additional non-local operations introduced by the quantities used in the correlations.

The general transport equation for the intermittency factor, γ, can be written as

$$\frac{\partial \rho u_j \gamma}{\partial x_j} = P_{\gamma 1} - E_{\gamma 1} + P_{\gamma 2} - E_{\gamma 2} + \frac{\partial}{\partial x_j}\left[\left(\mu + \frac{\mu_t}{\sigma_\gamma}\right)\frac{\partial \gamma}{\partial x_j}\right]. \tag{9}$$

This transport equation contains two production terms $P_{\gamma 1}$ and $P_{\gamma 2}$ and two dissipation terms $E_{\gamma 1}$ and $E_{\gamma 2}$ which are defined as follows:

$$P_{\gamma 1} = F_{\mathrm{length}} C_{a1} \rho S(\gamma F_{\mathrm{onset}})^{C_\alpha}, \quad E_{\gamma 1} = C_{e1} P_{\gamma 1}\gamma,$$
$$P_{\gamma 2} = C_{a2}\rho\Omega\gamma F_{\mathrm{turb}}, \quad E_{\gamma 2} = C_{e2} P_{\gamma 2}\gamma, \tag{10a–d}$$

where S is the strain rate magnitude, Ω is the vorticity magnitude, F_{length} is the empirical correlation that controls the length of the transition region. The production $P_{\gamma 1}$ is formulated as a function of F_{onset} which is controlled by the following functions:

$$F_{\mathrm{onset}} = \max[F_{\mathrm{onset2}} - F_{\mathrm{onset3}}; 0],$$
$$F_{\mathrm{turb}} = \exp[-(R_T/4)^4], \tag{11a, b}$$

$$F_{\text{onset2}} = \min[\max[F_{\text{onset1}}; F_{\text{onset1}}^4]; 2.0],$$

$$F_{\text{onset1}} = \frac{Re_v}{2.193 Re_{\theta c}}, \tag{12a, b}$$

$$F_{\text{onset3}} = \max[1 - (R_T/2.5)^3; 0],$$

$$Re_v = \frac{\rho S y^2}{\mu}, \quad R_T = \frac{\rho k}{\mu \omega}, \tag{13a–c}$$

where Re_v is the vorticity Reynolds number, Re_T is the viscosity ratio, y is the normal distance from the nearest wall, k is the turbulence kinetic energy, ω is the specific turbulence dissipation rate and $Re_{\theta c}$ is the critical momentum thickness Reynolds number. In this model, both F_{length} and $Re_{\theta c}$ are proprietary and are not given in the original papers.

The equation for the transition momentum thickness Reynolds number is designed to capture the non-local influence of the turbulence intensity which changes due to the decay of the turbulence kinetic energy in the freestream. It is formulated by treating the transition momentum thickness Reynolds number $Re_{\theta t}$ as a transported scalar quantity, $\widetilde{Re}_{\theta t}$, as shown in the following equation:

$$\frac{\partial \rho u_j \widetilde{Re}_{\theta t}}{\partial x_j} = P_{\theta t} + \frac{\partial}{\partial x_j}\left[\sigma_{\theta t}(\mu + \mu_t)\frac{\partial \widetilde{Re}_{\theta t}}{\partial x_j}\right]. \tag{14}$$

The source term $P_{\theta t}$ is defined as follows:

$$P_{\theta t} = C_{\theta t}(\rho/T)(Re_{\theta t} - \widetilde{Re}_{\theta t})(1.0 - F_{\theta t}), \tag{15}$$

$$T = \frac{500\mu}{\rho U^2},$$

$$F_{\theta t} = \min\left[\max\left[F_{\text{wake}} \cdot \mathrm{e}^{-\left(\frac{y}{\delta}\right)^4}; 1.0 - \left(\frac{C_{e2}\gamma - 1}{C_{e2} - 1}\right)^2\right]; 1.0\right], \tag{16a, b}$$

$$F_{\text{wake}} = \mathrm{e}^{-\left(\frac{Re_\omega}{10^5}\right)^2}, \quad Re_\omega = \frac{\rho \omega y^2}{\mu},$$

$$\delta = \frac{50\Omega y}{U}\delta_{BL}, \quad \delta_{BL} = \frac{15\theta_{BL}}{2}, \quad \theta_{BL} = \frac{\widetilde{Re}_{\theta t}\mu}{\rho U}, \tag{17a–e}$$

where U is the local velocity magnitude, T is the time scale for dimensional reasons and $F_{\theta t}$ is the blending function for turning off the influence of the production term $P_{\theta t}$ inside the boundary layer.

The model constants are $C_{a1} = 2.0$, $C_{e1} = 1.0$, $C_{a2} = 0.06$, $C_{e2} = 50.0$, $C_\alpha = 0.5$, $\sigma_\gamma = 1.0$, $\sigma_{\theta t} = 2.0$ and $C_{\theta t} = 0.03$. The onset of transition is determined from the empirical correlation of the transition momentum thickness Reynolds number, which is formulated as a function of the pressure gradient parameter, λ_θ, and the acceleration parameter, K, as follows:

$$Re_{\theta t} = 803.73(Tu + 0.6067)^{-1.027} F(\lambda_\theta, K), \tag{18}$$

$$F(\lambda_\theta, K) = \begin{cases} 1 - F_\lambda \mathrm{e}^{-Tu/3.0}; & \lambda_\theta \leqslant 0 \\ 1 + F_K(1 - \mathrm{e}^{-Tu/1.5}) & \\ \quad +0.556(1 - \mathrm{e}^{-23.9\lambda_\theta})\mathrm{e}^{-Tu/3.0}; & \lambda_\theta > 0 \end{cases}, \tag{19}$$

$$\lambda_\theta = \frac{\theta^2}{v}\cdot\frac{\mathrm{d}U}{\mathrm{d}s}, \quad K = \frac{v}{U^2}\cdot\frac{\mathrm{d}U}{\mathrm{d}s}, \tag{20a, b}$$

where Tu is the local turbulence intensity and θ is the momentum thickness. The functions, $F(\lambda_\theta, K)$, and the streamline acceleration, $\mathrm{d}U/\mathrm{d}s$, can be computed as follows:

$$F_\lambda = -10.32\lambda_\theta - 89.47\lambda_\theta^2 - 265.51\lambda_\theta^3, \tag{21}$$

$$F_K = 0.0962(K \cdot 10^6) + 0.148(K \cdot 10^6)^2 + 0.0141(K \cdot 10^6)^3, \tag{22}$$

$$\frac{\mathrm{d}U}{\mathrm{d}s} = \frac{u}{U}\cdot\frac{\mathrm{d}U}{\mathrm{d}x} + \frac{v}{U}\cdot\frac{\mathrm{d}U}{\mathrm{d}y}. \tag{23}$$

In order to obtain $Re_{\theta t}$, the calculation procedure must be performed iteratively, because both λ_θ and K are unknown. The steps of calculation are summarized as follows: (a) guess the initial value for θ_t ($\theta_t = 0$ is recommended), (b) calculate the λ_θ and K from Eqs. (20a) and (20b), respectively by setting $\theta = \theta_t$, (c) calculate the $F(\lambda_\theta, K)$, (d) calculate the $Re_{\theta t}$ from Eq. (18), and (e) calculate the θ_t from the definition of $\theta_t = (v/U)Re_{\theta t}$. The calculation may converge in a few iterations. To avoid the probably unstable computation during the iteration, the values of λ_θ, K, and $Re_{\theta t}$ obtained in each iteration should be bounded within the range of $-0.1 \leqslant \lambda_\theta \leqslant 0.1$, $-3 \times 10^{-6} \leqslant K \leqslant 3 \times 10^{-6}$ and $Re_{\theta t} \geqslant 20$.

This model has been calibrated for use in accordance with the SST turbulence model as follows:

$$\widetilde{P}_k = \gamma_{\text{eff}} P_k, \quad \widetilde{D}_k = \min(\max(\gamma_{\text{eff}}; 0.1); 1.0) D_k, \tag{24a, b}$$

where P_k and D_k are the production and destruction terms from the turbulence kinetic energy equation in the original SST turbulence model and γ_{eff} is the effective intermittency obtained from:

$$\gamma_{\text{eff}} = \max[\gamma; \gamma_{\text{sep}}], \tag{25}$$

$$\gamma_{\text{sep}} = \min\left[8.0 \max\left[\left(\frac{Re_v}{2.193 Re_{\theta c}}\right) - 1; 0\right] F_{\text{reattach}}; 5.0\right] F_{\theta t}, \tag{26}$$

$$F_{\text{reattach}} = \exp[-(R_T/15)^4]. \tag{27}$$

The SST model is modified by using the following blending function f_1:

$$f_1 = \max[f_{1,\text{orig}}; f_3], \tag{28}$$

$$f_3 = \exp\left[-(R_y/120)^8\right], \quad R_y = y k^{1/2}/v, \tag{29a, b}$$

where $f_{1,\text{orig}}$ is the original blending function responsible for switching between the k–ω and k–ε models.

The computation steps are given as follows: (a) solve the mean flow equations: the momentum equations and the continuity equation, (b) solve the turbulence model with a modified blending function f_1: the k-equation with modified production $\widetilde{P}_k$ and destruction $\widetilde{D}_k$ terms, and the ω-equation, and then compute the μ_t, (c) compute the empirical correlation of transition momentum thickness

Reynolds number $Re_{\theta t}$, Eq. (18), (d) solve the transition model: the γ- and $\widetilde{Re}_{\theta t}$ -equations.

The boundary conditions for the intermittency factor at freestream, outlet and walls are the zero flux ($\partial\gamma/\partial n = 0$). At inlet, $\gamma = 1.0$ is applied. For the $\widetilde{Re}_{\theta t}$, the boundary conditions at freestream, outlet and walls are zero flux ($\partial\widetilde{Re}_{\theta t}/\partial n = 0$). At inlet, the boundary condition can be specified by setting $\theta = 0$ (then $\lambda_\theta = 0$ and $F(\lambda_\theta, K) = 1$) and setting Tu with the value of freestream turbulence intensity at inlet and then substituting it into Eq. (18). The initial conditions for both γ and $\widetilde{Re}_{\theta t}$ are set to their inlet values all over the flow field.

3. Computation procedure

Three widely examined test cases: T3AM, T3A and T3B, which are classified as the low, moderate and high freestream turbulence intensity cases, respectively, are considered in the present paper where the transition is induced by the external freestream turbulence (bypass transition) rather than by the development of T–S waves (natural transition). All test cases are boundary-layer flows on a flat plate with a sharp leading edge under zero-pressure-gradient condition. Details of grid configuration and boundary conditions are shown in Fig. 1.

Computations are performed by an elliptic solver which solves the mean-flow equations, turbulence model and transition model using the second-order TVD-upwind scheme based on Van Leer's flux limiter (Van Leer, 1977) and the finite volume discretization. In computations, a variety of grid densities is explored by performing a grid-independent check, in which the grid spacing is decreased by half in both directions, and a mesh of 110 (streamwise) $\times$ 80 (expanding from wall to freestream) is adopted for all test cases. In all cases, the first node adjacent to the wall is located at y^+ below 0.3. Computations begin at $x = 15$ cm upstream of the plate leading edge. This is vital because it enables the uniform profiles of k and ω to be assigned. If one starts computations at the plate leading edge, the predicted transition point is strongly dependent on the assumptions made for the way k and ω vary across the boundary layer. As a consequence, a considerably reduced streamwise internodal spacing is needed in the vicinity of the plate leading edge (Craft et al., 1997).

In this work, incompressible flow is considered so that the fluid density and molecular viscosity are constant which are $1.2\ \mathrm{kg/m^3}$ and $1.8 \times 10^{-5}\ \mathrm{kg/m\,s}$, respectively. The boundary conditions for BC1, BC2, BC3 and BC4 are inlet, outlet, no-slip wall and freestream boundary conditions, respectively. In all computations, it should be noted that only the zero pressure gradient condition is of interest in this work so that the zero normal gradient of pressure has to be applied for all boundaries. The initial streamwise mean velocity profile is the Blasius velocity profile, and the inlet conditions are prescribed to reproduce the experimental decay of the freestream turbulence intensity. In this work, the isotropic turbulence is assumed. From this assumption, the inlet turbulence kinetic energy is obtained from the experimental inlet freestream turbulence intensity, and the inlet viscosity ratio is specified in order to mimic the experimentally measured decay of the freestream turbulence intensity. Hence, the inlet conditions of the turbulent variables are calculated from the following relationships:

$$\mu_t = R_\mu \mu, \quad k = (3/2)(Tu_0 \cdot U_0)^2, \quad \omega = \rho k/\mu_t, \qquad (30a\text{–}c)$$

where Tu_0 denotes the inlet freestream turbulence intensity (%), R_μ is the inlet viscosity ratio and U_0 is the inlet velocity.

It is found that the transition model of Menter et al. (2005) is incomplete because the unknown parameters F_{length} and $Re_{\theta c}$, which are formulated in functions of $\widetilde{Re}_{\theta t}$ relates to turbulence intensity Tu and pressure gradient function $F(\lambda_\theta, K)$, are proprietary and no information has been given in any previous publications. In order to use this model, those parameters must be specified. To predict the transition, the first two important characteristics of transition are where the onset of transition is and how long the length of transition is. To specify the onset of transition, one can do by comparing the computed momentum thickness Reynolds number with the critical value from the correlation. However, most correlations for specifying the onset of transition are usually related to the transition momentum thickness Reynolds number, $Re_{\theta t}$, not to the critical momentum thickness Reynolds number, $Re_{\theta c}$, and, in order to construct the formulation relating to $Re_{\theta c}$, some assumptions must be made. According to the process of transition, the transition starts from the linear instability of the T–S waves which gradually occur at the point where the Reynolds number equals $Re_{x,\mathrm{cr}}$, then the grown-up waves become non-linear and then break down, and then the formation of turbulent spots occurs at the point where the Reynolds number equals $Re_{x,\mathrm{tr}}$ which is always located

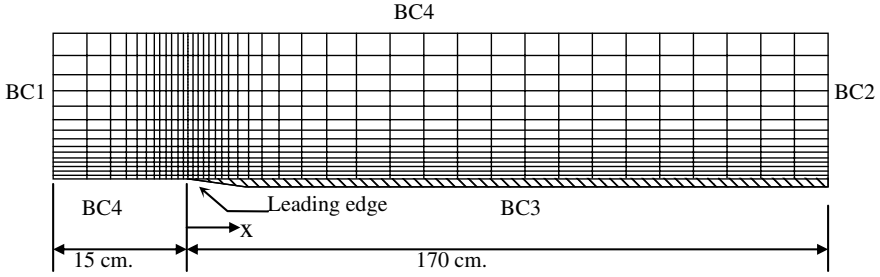

Fig. 1. Grid configuration and boundary conditions.

downstream of the critical point ($Re_{x,cr} \leqslant Re_{x,tr}$). Since all test cases are the transitional flow which is induced by the external freestream turbulence rather than by the development of T–S waves so that the behavior of transition is classified as bypass transition. In the bypass mode, the linear instability is ignored and the transition starts at the point where the turbulent spots first occur. Therefore, it is possible to approximate that the point where the instability first occurs and the point where the turbulent spots first occur are located at the same position. As a result, it is possible to approximate $Re_{x,cr} = Re_{x,tr}$ and is reasonable to assume that $Re_{\theta c} = Re_{\theta t}$. With this assumption, the parameter $Re_{\theta c}$ can be determined from the well-known correlations such as the correlations of Mayle (1991), Abu-Ghannam and Shaw (1980), etc. In the present work, the correlation of Menter et al. (2004), Eq. (18) which is a function of the turbulence intensity Tu and the pressure gradient function $F(\lambda_\theta, K)$, is adopted for finding $Re_{\theta c}$. Under the condition of zero pressure gradient, the influence of pressure gradient parameter has a small effect on the flow and can be neglected ($\lambda_\theta \approx 0$), and hence $F(\lambda_\theta, K) = 1$ is obtained. Since the critical point occurs upstream of the transition point, therefore, as already mentioned, it is also reasonable to assume that the turbulence intensity in Eq. (18) equals the upstream turbulence intensity, and in this work the freestream turbulence intensity at the leading edge, $Tu_{\infty,le}$, is adopted. After all, the correlation can be simplified and constructed as follows:

$$Re_{\theta c} = 803.73(Tu_{\infty,le} + 0.6067)^{-1.027}. \quad (31)$$

After specifying several values for the turbulence intensity $Tu_{\infty,le}$ in Eq. (31), the critical momentum thickness Reynolds number can be evaluated and plotted as illustrated in Fig. 2, and now only the F_{length} remains unknown. However, it is impossible to specify this parameter directly via any existing formula as can be done for the critical momentum thickness Reynolds number because there is no formulation for this parameter at all. One possible way to find out this parameter is to use the numerical experiment by carefully tuning it to match the numerical solutions with the published results of Menter et al. (2005). The values of F_{length} corresponding to $Re_{\theta c}$ are summarized in Tables 2a–c. It is found that only three correlations of Mayle (1991), Abu-Ghannam and Shaw (1980) and Menter et al. (2005) are capable of reproducing all test cases, while the correlation of Suzen and Huang (2000) is valid only for T3AM and T3B cases. The relation between both parameters is depicted in Fig. 3. These figures show a linear relation for T3AM case, and show the regions of valid values (highlighted region), which are bounded by the upper and lower limits of F_{length}, for T3A and T3B cases. According to Menter et al. (2004), the parameter F_{length} is formulated in function of $F_{length} = f(Tu, F(\lambda_\theta, K))$. However, due to the zero pressure gradient condition $F(\lambda_\theta, K) = 1$, $F_{length} = f(Tu)$ is obtained and in this work $F_{length} = f(Tu_{\infty,le})$ is assumed. The region of the validity of the F_{length}–$Tu_{\infty,le}$ relation is displayed with a highlighted area as illustrated in Fig. 2. In practice, one can formulate the relation of F_{length}–$Tu_{\infty,le}$ in several forms in this region, but only the form reasonable for the physical behavior of F_{length} is proposed here. In the intermittency transport equation, Eq. (9), F_{length} is incorporated in the equation via the production term. If the F_{length} is increased, the magnitude of the production term is increased leading to a higher value of the intermittency. This gives rise to an increase in the turbulence intensity whose influence induces an early transition onset and a rapid growth rate of transition leading to a shorter transition length. On the other hand, if F_{length} is decreased, the turbulence intensity is decreased whose influence induces a delayed transition onset and a slow growth rate of transition leading to a longer transition length. That means that the physical behavior of the F_{length} to control the transition length is an inverse process, that is, the larger F_{length} for the shorter transition length but the smaller F_{length} for the longer transition length. However, the magnitude of the F_{length} should

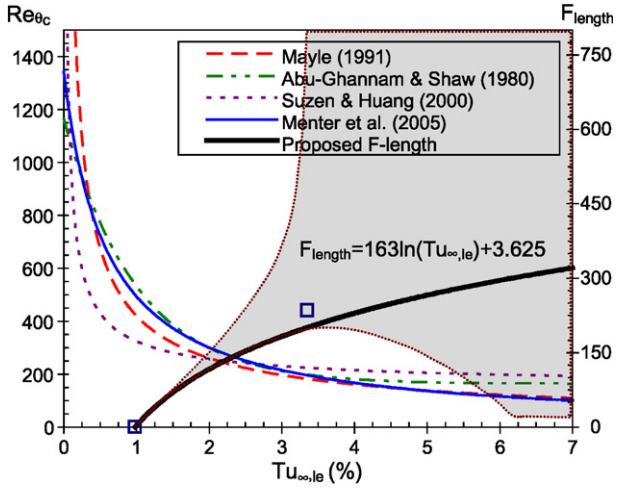

Fig. 2. Relations of $Re_{\theta c}$ and F_{length} with freestream turbulence intensity $Tu_{\infty,le}$.

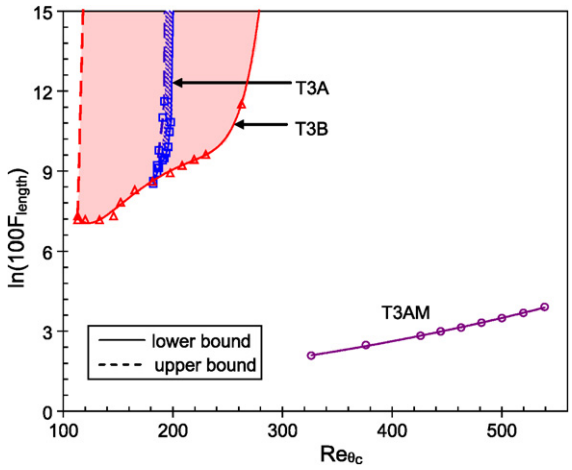

Fig. 3. Relation of F_{length} with $Re_{\theta c}$.

Table 1
Summary of all test case conditions

Case	U_0 (m/s)	Tu_0 (%)	R_μ	Re_L
T3AM	19.8	0.98	7.0	2.24×10^6
T3A	5.4	3.35	11.5	6.12×10^5
T3B	9.4	6.14	100.0	1.07×10^6

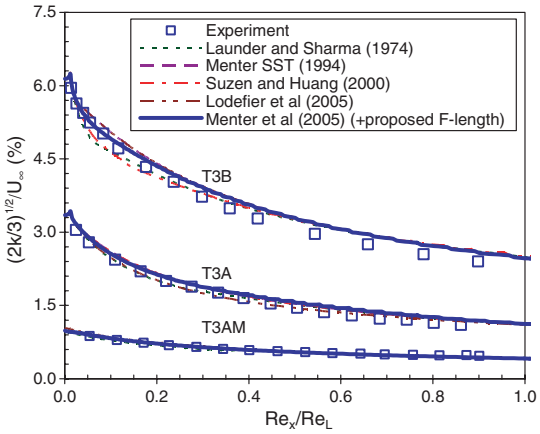

Fig. 4. Comparison of the measured freestream turbulence intensities with the numerical results.

be finite because the transition length must not be equal to zero when the transition occurs ($F_{\text{length}} = 0$ means the fully laminar flow occurs without transition, and $F_{\text{length}} \to \infty$ means the fully turbulent flow occurs without transition). As a result, the relation for F_{length} should be constructed with a growth rate and its growth rate should be a finite value when Tu approaches infinity, and the possible one under these constraints is proposed in a form of the logarithmic function as follows:

$$F_{\text{length}} = 163\ln(Tu_{\infty,\text{le}}) + 3.625. \tag{32}$$

However, this relation is reasonable for the zero pressure gradient condition in a range of freestream turbulence intensities of $0.98 < Tu_{\infty,\text{le}}\ (\%) < 7.0$.

Three transition models of different intermittency transport equations: models of Suzen and Huang (2000), Lodefier et al. (2003) and Menter et al. (2005), are used to predict the experimental test cases of Coupland (1993). These experimental data are specially selected to test the capability of transition models to predict the effect of freestream turbulence on the development of transition in the laminar boundary layer under the zero pressure gradient condition. Comparisons are also made for all test cases between these three transition models and two turbulence models, that is, the k–ε model of Launder and Sharma (1974), which has been known as the best model among all two-equation models for transitional flow, and the SST model of Menter (1994). The test cases are predicted using the conditions described in Table 1. The inlet conditions of turbulent variables are obtained by matching the decay of freestream turbulence intensity, $Tu_\infty = (2/3k)^{1/2}/U_\infty$, with the experimental data as shown in Fig. 4.

Table 2a
Summary of parameters $Re_{\theta c}$ and F_{length} for T3AM case

$Re_{\theta c}$	326 [2]	376	426 [3]	445	463	482	500 [1]	520	539 [4]	552
F_{length}	0.08	0.13	0.17	0.20	0.25	0.28	0.33	0.40	0.50	–

Table 2b
Summary of parameters $Re_{\theta c}$ and F_{length} for T3A case

$Re_{\theta c}$	183 [3]	186	189	191	192	193	196 [1]	197	198 [4]	202	224 [2]
F_{length}	50–55	75–100	100–300	120–900	130–1000	145–3000	>200	>350	>500	$>10^6$	–

4. Results and discussion

The predicted results of all considered models are compared with the experimental data of the momentum thickness Reynolds number based, Re_θ, the skin friction coefficient, C_f, the shape factor, H, the mean velocity profile scaled in wall units, u^+, the kinetic energy of turbulence, k, and the Reynolds shear stress, $-\overline{u'v'} = \nu_t \partial u/\partial y$. Fig. 5 shows the momentum thickness Reynolds number. This factor is directly related to the momentum thickness of the boundary layer which indicates the development of the boundary layer. In case of the boundary layer flow on a flat plate with zero pressure gradient, the boundary layer is laminar in the entrance region of the flat plate, and becomes transitional and then turbulent. The momentum thicknesses, from analysis, of laminar and turbulent boundary layers can be determined from $\theta_{\text{lam}} = 0.664x/Re_x^{1/2}$ and $\theta_{\text{tur}} = (7/72)0.16x/Re_x^{1/7}$ which are the upper and lower dash lines, respectively, so that the values for the transitional boundary layer can be found in the region between both dash lines. In the profile of the momentum thickness Reynolds number along the flat plate, the transition starts at the point where the profile deviates from the laminar line, and ends at the point where the profile touches the turbulence line. The experimental data indicate that the transition starts at Reynolds numbers of 1.40×10^6, 1.35×10^5 and 5.90×10^4 corresponding to the momentum thickness Reynolds numbers of 810, 272 and 180 for T3AM, T3A and T3B cases, respectively. At the end of transition, the experimental data show that the transition ends at the Reynolds number of 3.09×10^5 and 1.25×10^5, or the momentum thickness Reynolds number of 628 and 337, for T3A and T3B cases, respectively, while for the T3AM case the development of the boundary layer from laminar to turbulent flow is not yet complete within the length of the flat plate, 170 cm, and hence no ending point of transition appears.

Fig. 6 shows the skin friction coefficient, which is an important factor for indicating the starting and ending points of transition, and also indicates the growth rate

Table 2c
Summary of parameters $Re_{\theta c}$ and F_{length} for T3B case

$Re_{\theta c}$	113 [1]	120 [3]	133	146	152	165 [4]	181	198 [2]	208	219	230	263
F_{length}	>13	>13	>13	>15	>25	>40	>55	>75	>100	>125	>150	>1000

[1] $Re_{\theta t} = 803.73(Tu_{\infty,le} + 0.6067)^{-1.027}$, Menter et al. (2005).
[2] $Re_{\theta t} = [120 + 150(Tu_{\infty,t})^{-2/3}]\coth[4(0.3 - 10^5 K_t)]$, Suzen and Huang (2000).
[3] $Re_{\theta t} = 420(Tu_{\infty,le})^{-0.69}$, Mayle (1991).
[4] $Re_{\theta t} = 163 + \exp(6.91; - Tu_{\infty,le})$, Abu-Ghannam and Shaw (1980).
Note: The $Re_{\theta c}$ above is determined based on the assumption of $Re_{\theta c} = Re_{\theta t}$.

characteristic of transition leading to the length of transition to be found. In case of the flat plate boundary layer flow under a zero pressure gradient condition, the analytic skin friction coefficient for laminar and turbulent flows can be determined from $c_f = 0.664/Re^{1/2}$ and $c_f = 0.027/Re^{1/7}$, respectively, displayed by the dash lines in Fig. 6. The variation of the skin friction coefficient along the flat plate is usually displayed with respect to the Reynolds number, and the linear-scale plot is displayed in this work. The start and end of transition occur at the points where the skin friction coefficient profile deviates from and approaches to the laminar and turbulent values respectively, and the variation between these two points indicates the growth rate and length of transition (the more the rapid growth rate; the shorter the transition length). Fig. 7 displays the shape factor, defined as the ratio of the displacement thickness to the momentum thickness in the boundary layer ($H = \delta^*/\theta$), describes the influence of the freestream turbulent eddies on transition. Moreover, it indicates if the boundary layer is separated or has the tendency to separate. However, in zero-pressure-gradient cases considered here, the shape factor indicates the region where the boundary layer tends to be turbulent. A decrease in the shape factor implies that the transition to turbulent boundary layer is about to occur. For the flat plat boundary layer flow under a zero pressure gradient condition, from analysis, the shape factors for laminar and turbulent boundary layers are about 2.6 and 1.4, respectively, and the values between these two limits are for the transitional boundary layer. Fig. 8 shows the mean velocity profile scaled in wall units in the pre-transition (laminar), transition, and post-transition (turbulent) regions with respect to the normal distance scaled in wall units, y^+. For T3AM/T3A/T3B cases, the experimental data of the pre-transition, transition and post-transition regions are obtained at the locations corresponding to the Reynolds numbers, $Re_x = U_\infty x/\nu$, of $6.42\times10^5/10.06\times10^4/4.31\times10^4$, $11.73\times10^5/20.35\times10^4/8.93\times10^4$ and $18.28\times10^5/30.93\times10^4/18.85\times10^4$, or the distance from the leading edge of 495/295/70, 895/595/145 and 1395/895/295 mm, respectively. At the same locations of the mean velocity profile, the kinetic energy of turbulence and the Reynolds shear stress, which are normalized by the inlet velocity, U_0, are shown in Figs. 9 and 10 respectively.

The SST turbulence model of Menter (1994) always produces a fully turbulent feature and cannot detect any effect of transition. This model gives the immediate transition to turbulence at the leading edge of the flat plate showing almost no laminar zone. This is because the predicted profile of momentum thickness Reynolds number deviates from the laminar line and reaches the turbulent value at the leading edge location (Fig. 5). As a result, the skin friction coefficient predicted by this model follows the turbulent skin friction coefficient (Fig. 6), and the immediate decay of the shape factor at the leading edge is found for all three test cases (Fig. 7). The model always gives fully turbulent velocity profiles in all regions for all three cases (Fig. 8). The model shows the under-predicted profiles for pre-transition and transition regions but gives a good predicted result for the post-transition region. However, in the post-transition region of T3AM case, the model gives the under-predicted result because the low freestream turbulence intensity probably makes the flow become natural transition and there is no appearance of the fully turbulent boundary layer in this region. The model gives the predicted kinetic energy of turbulence in good agreement with the experimental data in cases of moderate and high freestream turbulence intensity for the post-transition region, gives the fairly well result for the pre-transition region and gives the over-predicted result in case of low freestream turbulence intensity because the isotropic turbulence is assumed in the computation (Fig. 9). For the Reynolds shear stress, the model gives the over-predicted result with the peak point at about $y/\delta \approx 0.15$ for all three cases (Fig. 10).

With the k–ε model of Launder and Sharma (1974), the predicted momentum thickness Reynolds number is located in the transition region and the deviation of its profile from the laminar line does not appear at the leading edge for all three cases (Fig. 5). This implies that this model is able to predict the transitional flow. The model gives the laminar solution from the leading edge to the transition onset, and gives satisfactorily the onset location of transition with a rapid growth rate of transition to turbulence leading to a shorter transition length when compared with the experimental data (Figs. 6 and 7). In the pre-transition region, the model gives satisfactorily the results of the velocity profiles compared with the experimental data for all test cases. In the transition region, the under-predicted velocity profiles are obtained for all cases because too much turbulence is produced by the model. In the post-transition region, the model gives the under-predicted

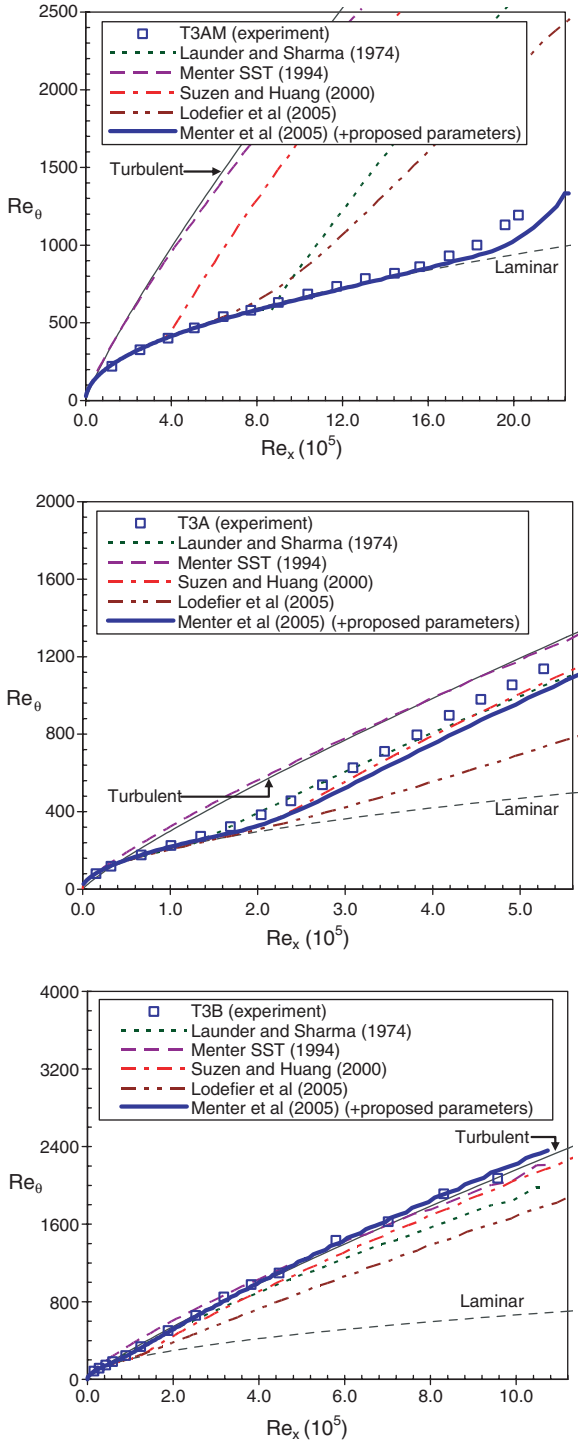

Fig. 5. Momentum thickness Reynolds number for T3AM (top), T3A (middle), and T3B (bottom) cases.

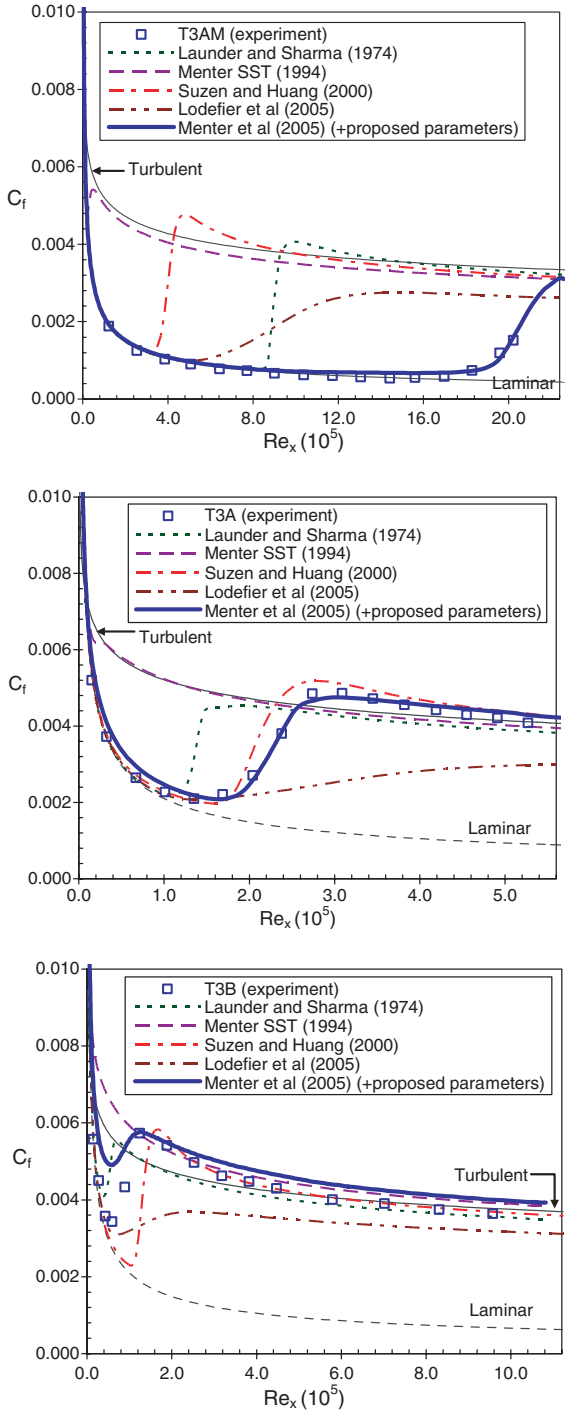

Fig. 6. Skin friction coefficient for T3AM (top), T3A (middle), and T3B (bottom) cases.

velocity profiles for the case of low freestream turbulence intensity because the boundary layer is not fully turbulent at this position, but for the cases of moderate and high freestream turbulence intensities the results agree well with the experimental data (Fig. 8). For the kinetic energy of turbulence (Fig. 9), the model gives the under-predicted result in the pre-transition region and gives satisfactory result in the post-transition region. In the transition region, the model gives the over-predicted result in case of low freestream turbulence intensity because the turbulence effect is early produced by the model, while, for the other cases, the reasonable results are obtained. The model always gives the over-predicted result for the Reynolds shear stress for all test cases. The profiles exhibited an over-shoot between $0.1 < y/\delta < 0.5$ for the pre-transition

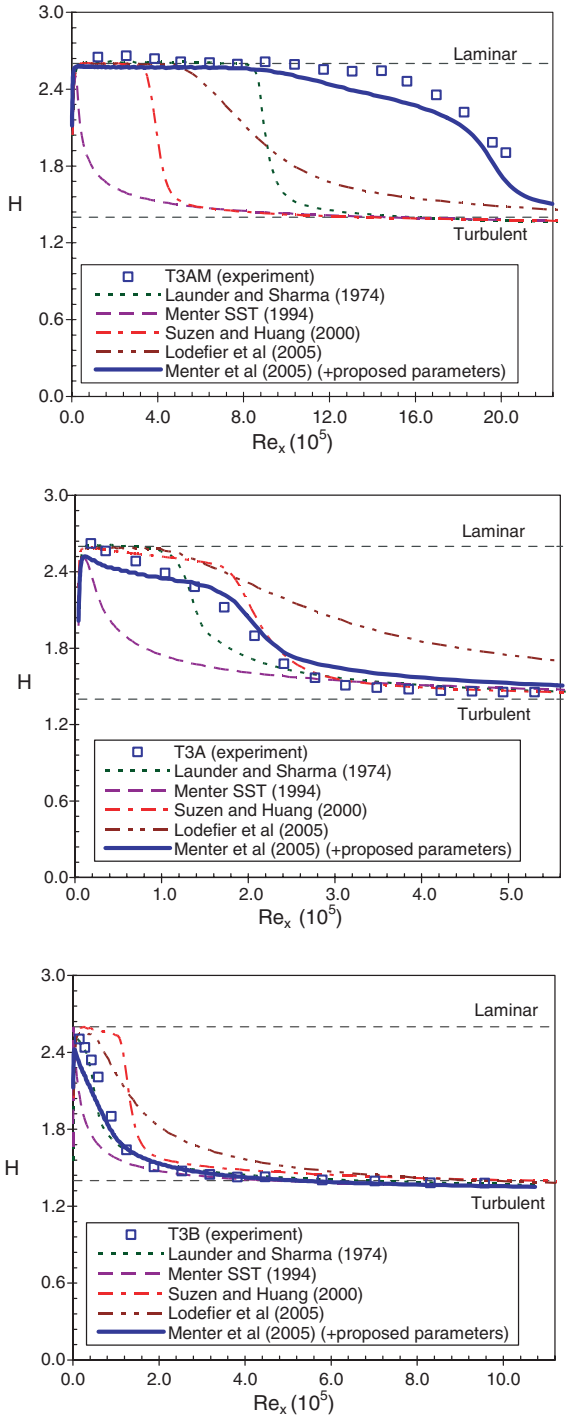

Fig. 7. Shape factor for T3AM (top), T3A (middle), and T3B (bottom) cases.

region and $0.1 < y/\delta < 0.75$ for the transition and post-transition regions (Fig. 10).

With the model of Suzen and Huang (2000), the deviation of the momentum thickness Reynolds number profile from the laminar line shows an early onset of transition in the case of low freestream turbulent intensity and shows a delayed onset of transition in the cases of moderate and high freestream turbulent intensities (Fig. 5). In all cases, a rapid variation of the skin friction coefficient with a slight overshoot at the end of the transition region is obtained which implies a rapid growth rate of transition produced by the model leading to a shorter transition length (Fig. 6). The model predicts a constant shape factor at the laminar value of 2.6 from the leading edge toward the transition onset. The reason is that the intermittency factor γ in the upstream location of the transition onset is set to a small value so that the model cannot be activated by the freestream turbulence intensity (Fig. 7). In the pre-transition region, for the low freestream turbulent intensity, the model gives the under-predicted velocity profile which is a result of an early transition onset prediction leading to too early turbulence production. However, for moderate and high freestream turbulence intensities the model gives reasonable results compared with the experimental data. In the transition region, the predicted velocity profile agrees fairly well with the experimental data in the case of moderate freestream turbulence intensity, but for low and high freestream turbulence intensities the model gives under- and over-predicted results respectively. In the post-transition region, the model gives the under-predicted velocity profile for the case of low freestream turbulence intensity because the boundary layer is not fully turbulent at this position, and gives good results in the cases of moderate and high freestream turbulence intensities (Fig. 8). The profiles of the kinetic energy of turbulence are over-predicted before the beginning of the transition region and the agreement is improved at locations further downstream (Fig. 9). For the Reynolds shear stress (Fig. 10), the over-predicted result is obtained in case of low freestream turbulence intensity with the same magnitude as given by the SST model because the early production of the turbulence appears. For moderate and high freestream turbulence intensities, the model simulates the under-predicted result before the beginning of transition and then gives the over-predicted result at the location further downstream. However, in case of high freestream turbulence, the under-predicted result of the Reynolds shear stress is obtained in the transition region because of the delayed transition.

With the model of Lodefier et al. (2003), the model gives an early onset of transition in the case of low freestream turbulence intensity and gives a delayed onset of transition in the cases of moderate and high freestream turbulence intensities (Fig. 5). The model predicts a slow growth rate of the transition with the under-predicted skin friction coefficient for all three cases because the model tends to be laminar and cannot reach the turbulent state (Fig. 6). For the shape factor, this model cannot detect the fully turbulent behavior for all three cases (Fig. 7). For the velocity profiles (Fig. 8), in the pre-transition region, the model gives reasonable results for all cases, but in the transition and post-transition regions, the model gives the under-predicted result in the case of low freestream turbulence intensity and gives over-predicted results in the cases of moderate and high freestream turbulence intensities. The

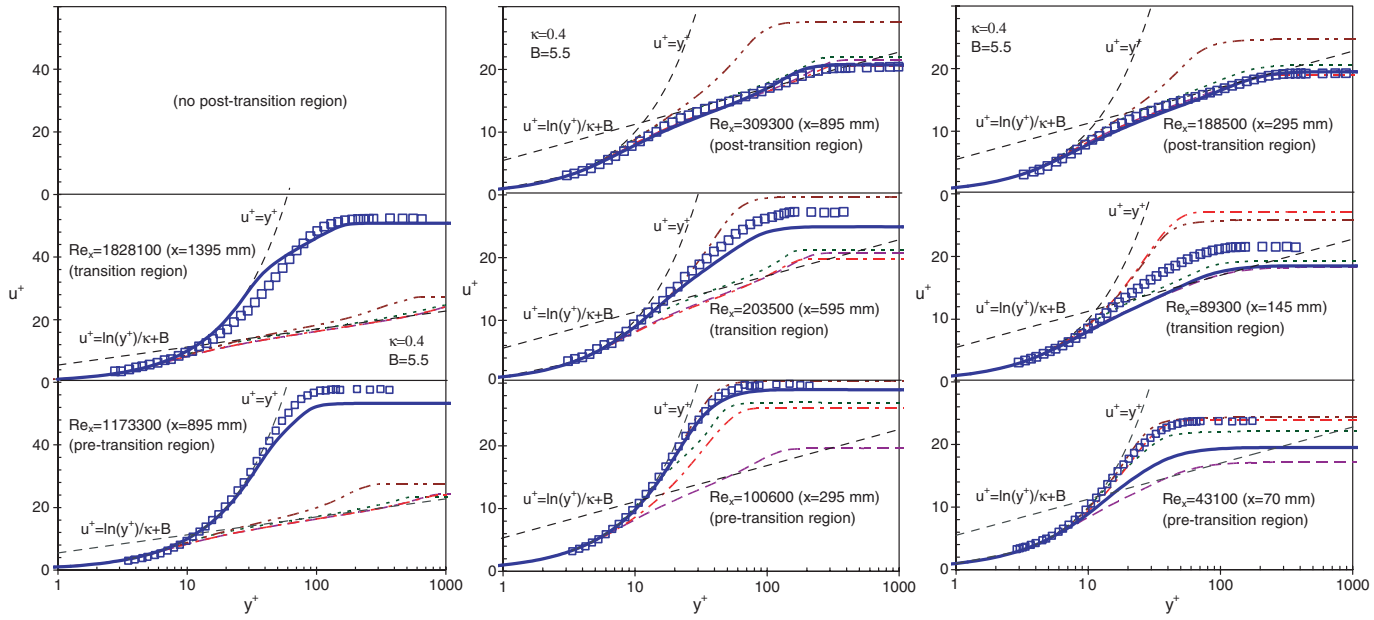

Fig. 8. u^+ vs. y^+ for T3AM (top left), T3A (top right), and T3B (bottom left). Experimental data: □. Predicted results: (---) Launder and Sharma (1974), (——) Menter SST (1994), (—·—) Suzen and Huang (2000), (—··—) Lodefier et al. (2003) and (——) Menter et al. (2005) (+ proposed parameter).

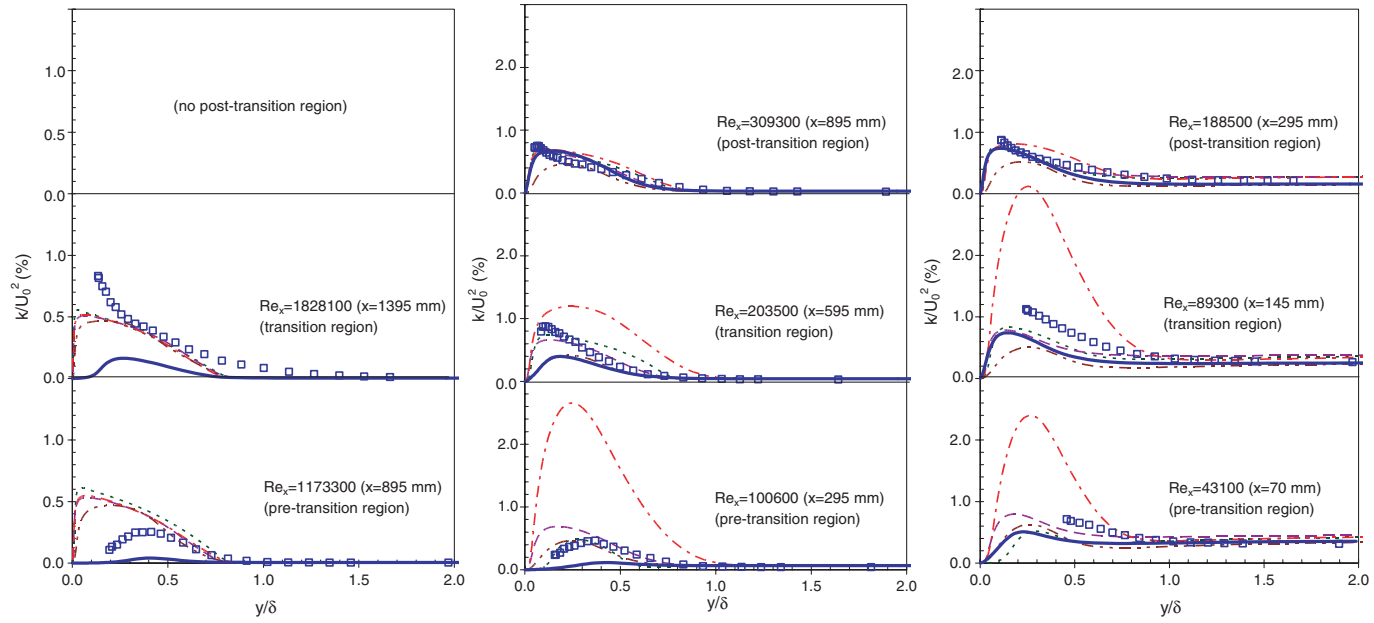

Fig. 9. k/U_0^2 vs. y/δ for T3AM (top left), T3A (top right), and T3B (bottom left). Experimental data: □. Predicted results: (---) Launder and Sharma (1974), (——) Menter SST (1994), (—·—) Suzen and Huang (2000), (—··—) Lodefier et al. (2003) and (——) Menter et al. (2005) (+ proposed parameter).

model gives reasonable results of the kinetic energy of turbulence in the pre-transition region for all cases but gives the under-predicted result at the location further downstream because the fully turbulent behavior cannot be produced by this model within the length of the flat plate (Fig. 9), leading to the under-predicted result of the Reynolds shear stress (Fig. 10).

With the model of Menter et al. (2005), this transition model gives good predicted results for the boundary layer development (Fig. 5). In comparison of the computed skin friction coefficient with the experimental data, the model gives the satisfactory transition onset and length for the cases of low and moderate freestream turbulence intensities, but gives a too early onset of transition and an unsatisfactory transition length for the case of high freestream turbulence intensity (Fig. 6). In comparison of the shape factor, the model is able to simulate the diffusion of turbulent eddies into the underlying laminar boundary layer

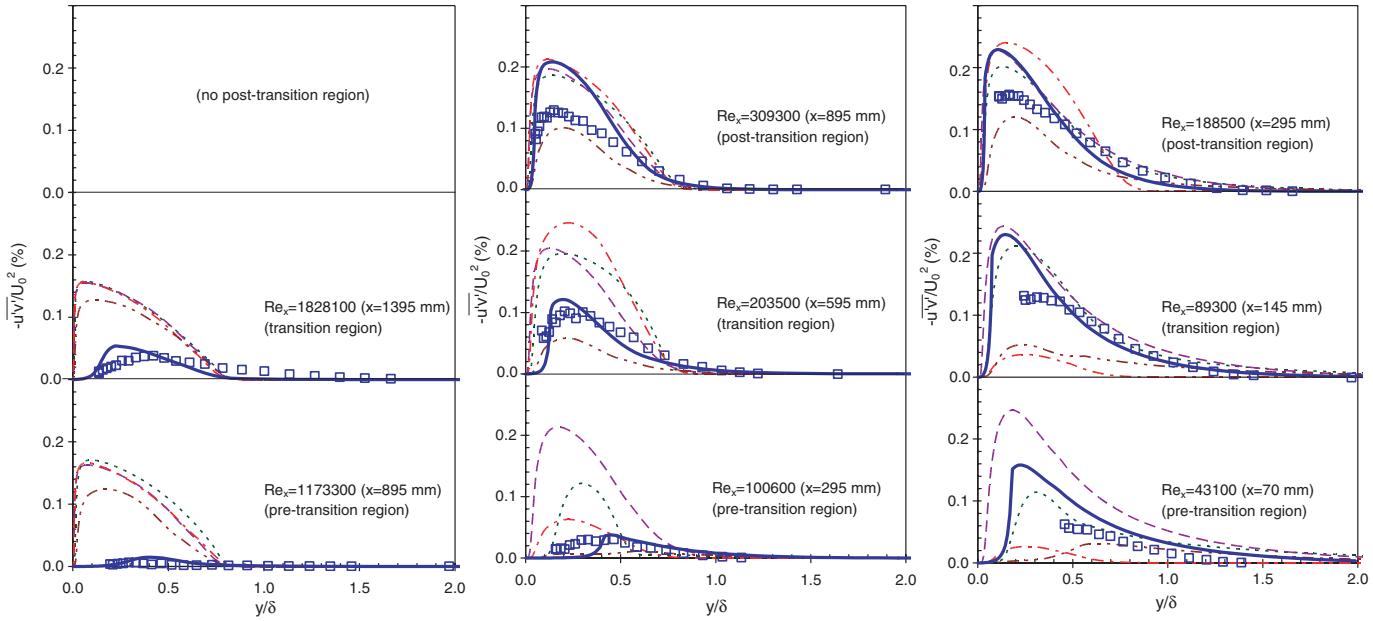

Fig. 10. $-\overline{u'v'}/U_0^2$ vs. y/δ for T3AM (top left), T3A (top right), and T3B (bottom left). Experimental data: □. Predicted results: (---) Launder and Sharma (1974), (——) Menter SST (1994), (—·—) Suzen and Huang (2000), (—··—) Lodefier et al. (2003) and (——) Menter et al. (2005) (+ proposed parameter).

because the intermittency factor at the upstream location of transition onset is set to unity so that a decrease in the measured shape factor starting from the leading edge is well predicted. In the cases of low and moderate freestream turbulence intensities, the results agree well with the experimental data, and for the high freestream turbulence intensity case, the model gives the immediate decay of the shape factor at the leading edge because the model cannot completely stop the behavior of the laminar boundary layer in the pre-transition region, and the turbulence effects occur near the leading edge region (Fig. 7). In comparison of the velocity profile, the model gives satisfactory results compared with the experimental data in all regions and for all cases (Fig. 8). For the kinetic energy of turbulence (Fig. 9), the model gives the under-predicted result in all cases for the pre-transition and transition regions, and predicts satisfactory results for the post-transition region. For the Reynolds shear stress (Fig. 10), the results agree well with the experimental data for the low and moderate freestream turbulence intensity cases, and the over-predicted result is obtained for the high freestream turbulence intensity case because the too early transition is produced.

The capability among the models considered to predict the transition is discussed. The SST turbulence model cannot predict the influence of the transitional flow because it has been developed from the high-Reynolds-number turbulence model without any wall damping function to reproduce the viscous sublayer behavior so that it always produces the fully turbulent flow. The low-Reynolds-number turbulence model of Launder and Sharma (1974) with the wall damping function can capture the transition behavior but it predicts well merely in case of high freestream turbulence level because its damping function has been developed to handle the near-wall region of turbulent flow, not calibrated for transition prediction, but produce the transition location as a by-product of their viscous sublayer formulation. The model of Suzen and Huang (2000) is proper for the transition prediction in the range of moderate freestream turbulence intensity. This model always predicts the laminar behavior upstream of the transition onset because the intermittency at the inlet boundary is specified with the small value, therefore the influence of the freestream turbulence affecting the transition is ignored. The onset correlation of Suzen and Huang (2000) seems to be not accurate enough for predicting the onset location in which case it predicts the early start of transition for the low freestream turbulence intensity case and gives the delayed onset of transition for the high freestream turbulence intensity case. The model of Lodefier et al. (2003) is too much sensitive to the computational stability due to the improper form of the diffusion coefficient μ_ζ in the transport equation of the freestream intermittency. Furthermore, the accurate prediction with this model is significantly dependent on the corresponding value of the starting function F_s, which is related to the intensity of the freestream turbulence, specified for the computation. This function is not a continuous function and not a generalized form and its value is considered on the case-by-case basis. A main disadvantage of both Suzen and Huang (2000) and Lodefier et al. (2003) models is that they are strongly non-local in their formulation because they require the computation of boundary layer thickness parameters and transition-length from a given point which depend on the specific geometry and grid set-up. The model of Menter et al. (2005) has been constructed based on the empirical correlation without the physical processes of

the transition. The model generates the whole intermittency from the influence of the freestream turbulence, while the influence of the turbulent spots on the near-wall intermittency is ignored. The model is effectively used for predicting the transition in the range of freestream turbulence below the high level because the specification of the intermittency at the inlet equals to one leading to the allowance of the freestream to build up the turbulence effect from the leading edge. As a result, for high freestream turbulence intensity, the model always predicts the early start of transition.

5. Conclusion

The proposed F_{length} and $Re_{\theta c}$ based on the assumption of $Re_{\theta c} = Re_{\theta t}$ work well with the model of Menter et al. (2005) to give good agreement in predicting the transition. Three transition models with intermittency transport equations are implemented and their abilities are assessed: (1) the model of Suzen and Huang (2000) which interacts with the turbulence model via the diffusion part of the mean flow equations, (2) the model of Lodefier et al. (2003) which interacts with the turbulence model via the diffusion part of the mean flow equations and the production terms of the turbulence kinetic energy and specific turbulence dissipation rate, $P_{k/\omega}$, and (3) the model of Menter et al. (2005) which interacts with the turbulence model via the production term of the turbulence kinetic energy, P_k. All these models are used in conjunction with the SST turbulence model to predict the flat plate boundary-layer flow with zero pressure gradient and three different freestream turbulence intensities corresponding to the conditions of T3AM, T3A and T3B experiments by Coupland (1993). The computed results show that (1) the model of Lodefier et al. (2003) gives unsatisfactory results for all cases, (2) the model of Suzen and Huang (2000) gives good results at the moderate freestream turbulence intensity, (3) the model of Menter et al. (2005) gives good results over a range of low and moderate freestream turbulence intensities, (4) the k–ε turbulence model of Launder and Sharma (1974) gives the satisfactory onset of transition but predicts the transition length too short and, moreover, this model is appropriate for use in simulating the transition at high freestream turbulence intensity, and (5) the SST turbulence model of Menter (1994) gives fully turbulent results for all cases and cannot detect any transition effect.

Acknowledgements

This research is supported by the Thailand Research Fund (TRF) for the Senior Scholar Professor Dr. Pramote Dechaumphai, and the authors would like to personally thank Dr. Y.B. Suzen, Dr. F.R. Menter, Dr. Koen Lodefier and Dr. Rene Pecnik for their helpful discussion and papers during the course of this work. We also would like to thank Institute for Mathematical Sciences (IMS), National University of Singapore (NUS) for financially supporting our stay during the "Wall-Bounded and Free-Surface Turbulence and Its Computation" workshops on "Transition & Turbulence Control" and "Developments in Navier–Stokes Equations & Turbulence Research" (7–17 December 2004).

References

Abid, R., 1993. Evaluation of two-equation turbulence models for predicting transitional flows. J. Eng. Sci. 31, 831–840.

Abu-Ghannam, B.J., Shaw, R., 1980. Natural transition of boundary layer: the effects of turbulence, pressure gradient, and flow history. J. Mech. Eng. Sci. 22, 213–228.

Baek, S.G., Chung, M.K., 2001. k–ε Model for predicting transitional boundary-layer flows under zero-pressure gradient. AIAA 39, 1699–1705.

Cho, J.R., Chung, M.K., 1992. A k–ε–γ equation turbulence model. J. Fluid Mech. 237, 30–322.

Coupland, J., 1993. ERCOFTAC Classic Database. http://cfd.me.umist.ac.uk/ercoftac/ (accessed on May 2005).

Craft, T.J., Launder, B.E., Suga, K., 1997. Prediction of turbulence transition phenomena with a nonlinear eddy-viscosity model. J. Heat Fluid Flow 18, 15–28.

Dhawan, S., Narasimha, R., 1958. Some properties of boundary layer during the transition from laminar to turbulent flow motion. J. Fluid Mech. 3, 418–436.

Langtry, R.B., Menter, F.R., 2005. Transition modeling for general CFD applications in aeronautics. AIAA 2005-522.

Lardeau, S., Li, N., Leschziner, M.A., 2005. LES of transitional boundary layer at high free-stream turbulence intensity and implications for RANS modelling, pp. 431–436.

Launder, B.E., Sharma, B., 1974. Application of the energy dissipation model of turbulence to the calculation of flow near a spinning disk. Lett. Heat Mass Transfer 1, 131–138.

Lodefier, K., Merci, B., De Langhe, C., Dick, E., 2003. Transition modeling with the SST turbulence model and intermittency transport equation. ASME Turbo Expo, Atlanta, GA, USA, June 16–19.

Mayle, R.E., 1991. The role of laminar-turbulent transition in gas turbine engines. ASME J. Turbomach. 113, 509–537.

Menter, F.R., 1994. Two-equation eddy-viscosity turbulence models for engineering applications. AIAA 32, 1598–1605.

Menter, F.R., Esch, T., Kubacki, S., 2002. Transition modelling based on local variables. In: Rodi, W., Fueyo, N. (Eds.), Engineering Turbulence Modelling and Experiments, vol. 5, pp. 555–564.

Menter, F.R., Langtry, R.B., Likki, S.R., Suzen, Y.B., Huang, P.G., Volger, S., 2004. A correlation based transition model using local variables: Part I – Model formulation. Proceedings of ASME Turbo Expo 2004, Power for Land, Sea, and Air, June 14–17, Vienna, Austria.

Menter, F.R., Langtry, R.B., Volker, S., Huang, P.G., 2005. Transition modelling for general purpose CFD codes. ERCOFTAC International Symposium Engineering Turbulence Modelling and Measurements.

Steelant, J., Dick, E., 1996. Modelling of bypass transition with conditioned Navier–Stokes equations coupled to an intermittency transport equation. J. Numer. Methods Fluids 23, 193–220.

Suzen, Y.B., Huang, P.G., 2000. Modeling of flow transition using an intermittency transport equation. J. Fluids Eng. 122, 273–284.

Suzen, Y.B., Huang, P.G., 2001. Predictions of separated and transitional boundary layers under low pressure turbine airfoil conditions using an intermittency transport equation. In: AIAA 200-0446, 39th AIAA Aerospace Sciences Meeting & Exhibit, Reno, NV, January 8–11.

Van Leer, B., 1977. Towards the ultimate conservative difference scheme. iv. a new approach to numerical convection. J. Comput. Phys. 23, 276–299.